Acta Cryst E CRYSTALLOGRAPHIC COMMUNICATIONS

ISSN 2056-9890

A 1:2 co-crystal of 2,2′-dithiodibenzoic acid and benzoic acid: crystal structure, Hirshfeld surface analysis and computational study

Sang Loon Tan‡ and Edward R. T. Tiekink*

Research Centre for Crystalline Materials, School of Science and Technology, Sunway University, 47500 Bandar Sunway, Selangor Darul Ehsan, Malaysia. *Correspondence e-mail: edwardt@sunway.edu.my

Received 30 November 2018
Accepted 1 December 2018

Edited by W. T. A. Harrison, University of Aberdeen, Scotland

‡ Additional correspondence author, e-mail: alant@sunway.edu.my.

Keywords: crystal structure; dithiodibenzoic acid; benzoic acid; hydrogen bonding; computational chemistry.

CCDC reference: 1882556

Supporting information: this article has supporting information at journals.iucr.org/e

The asymmetric unit of the title 1:2 co-crystal, $C_{14}H_{10}O_4S_2{\cdot}2C_7H_6O_2$, comprises half a molecule of dithiodibenzoic acid [systematic name: 2-[(2-carboxyphenyl)-disulfanyl]benzoic acid, DTBA], as the molecule is located about a twofold axis of symmetry, and a molecule of benzoic acid (BA). The DTBA molecule is twisted about the disulfide bond [the C—S—S—C torsion angle is −83.19 (8)°] resulting in a near perpendicular relationship between the benzene rings [dihedral angle = 71.19 (4)°]. The carboxylic acid group is almost co-planar with the benzene ring to which it is bonded [dihedral angle = 4.82 (12)°]. A similar near co-planar relationship pertains for the BA molecule [dihedral angle = 3.65 (15)°]. Three-molecule aggregates are formed in the crystal whereby two BA molecules are connected to a DTBA molecule via hydroxy-O—H···O(hydroxy) hydrogen bonds and eight-membered $\{\cdots HOC{=}O\}_2$ synthons. These are connected into a supramolecular layer in the *ab* plane through C—H···O interactions. The interactions between layers to consolidate the three-dimensional architecture are π–π stacking interactions between DTBA and BA rings [inter-centroid separation = 3.8093 (10) Å] and parallel DTBA-hydroxy-O···π(BA) contacts [O···ring centroid separation = 3.9049 (14) Å]. The importance of the specified interactions as well as other weaker contacts, *e.g.* π–π and C—H···S, are indicated in the analysis of the calculated Hirshfeld surface and interaction energies.

1. Chemical context

Molecular recognition represents an essential aspect in the crystal engineering of co-crystals as it dictates how supramolecular aggregates are formed, whether through shape, size or functional complementarity, to give a distinct connectivity and pattern (Meng *et al.*, 2008). To date, various supramolecular frameworks comprising homo-synthons, occurring between the same functional groups, as well as hetero-synthons, occurring between disparate functional groups, have been described. Molecules with carboxylic acid functionality remain at the forefront of co-crystal technology based on hydrogen-bonded synthons (Duggirala *et al.*, 2015). Despite expectations to the contrary, the carboxylic acid···carboxylic acid homo-synthon, *i.e.* association through the formation of an eight-membered $\{\cdots HOC{=}O\}_2$ synthon, only forms in about one-third of structures where they potentially can occur (Allen *et al.*, 1999). The remaining structures of carboxylic acids are dominated by hetero-synthons involving carboxylic acid with other functional groups, such as a pyridyl residue (Shattock *et al.*, 2008). This relatively low probability is due to competing supramolecular interactions that hinder the

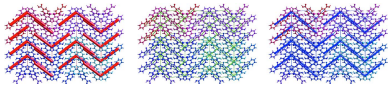

formation of the homosynthon (Steiner, 2001). A related issue concerns the formation of co-crystals involving different carboxylic acids (Seaton, 2011). Here, different crystalline outcomes may be envisaged and in terms of co-crystals, co-crystals involving the same molecules associating via a symmetric carboxylic acid homosynthon might be isolated, or a co-crystal comprising different molecules, via a non-symmetric homo-synthon might be formed. In this context, in a recent study, the characterization of the 2:1 co-crystal between 2,2′-dithiodibenzoic acid (DTBA) and 3-chlorobenzoic acid showed the formation of a homo-synthon between two DTBA molecules with each of the terminal carboxylic acid residues of the two-molecule aggregate engaged in non-symmetric homo-synthons with two 3-chlorobenzoic acid molecules, giving rise to a hydrogen-bonded four-molecule aggregation pattern (Tan & Tiekink, 2019). In continuation of these studies, herein, the crystal and molecular structures of the title 1:2 co-crystal of DTBA and benzoic acid (BA) are described as well as an analysis of the calculated Hirshfeld surface and the calculation of some specific interaction energies through a computational chemistry approach.

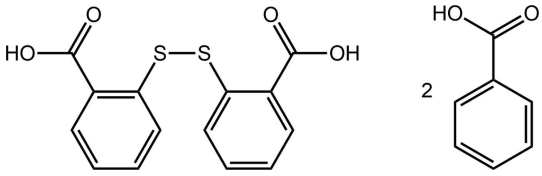

2. Structural commentary

The title co-crystal (I) was the result of crystallization of a powder resulting from the solvent-assisted (methanol) grinding of a 1:1 mixture of 2-thiobenzoic acid and benzoic acid. X-ray crystallography showed the asymmetric unit of the resultant crystals to comprise half a molecule of 2,2′-dithiodibenzoic acid (DTBA), as this is disposed about a crystallographic twofold axis of symmetry, Fig. 1(*a*), and a molecule of benzoic acid (BA) in a general position, Fig. 1(*b*). Such oxidation of the original 2-thiobenzoic acid to DTBA is well known in co-crystallization studies (Broker & Tiekink, 2007; Gorobet *et al.*, 2018). In terms of stoichiometry, the formation of the title 1:2 co-crystal is consistent with the 1:1 stoichiometry of the original grinding experiment.

The twofold-symmetric DTBA molecule is twisted about the disulfide bond with the C3—S1—S1^{i}—C3^{i} torsion angle being −83.19 (8)°; symmetry operation (i): $1-x, y, \frac{1}{2}-z$. This almost orthogonal disposition is also seen in the dihedral angle between the benzene rings of 71.19 (4)°. The presence of a carboxylic acid group is readily confirmed by the disparity in the C1—O1, O2 bond lengths, *i.e.* 1.317 (2) and 1.229 (2) Å, respectively. This group is practically co-planar with the benzene ring to which it is bonded, as seen in the dihedral angle of 4.82 (12)°. This co-planar arrangement allows for a significant intramolecular S←O interaction, *i.e.* S1···O2 = 2.6712 (12) Å, as the carbonyl-O2 atom is orientated towards a disulfide-S1 atom (Nakanishi *et al.*, 2007).

Table 1
Hydrogen-bond geometry (Å, °).

D—H···A	D—H	H···A	D···A	D—H···A
O1—H1O···O4	0.88 (3)	1.74 (3)	2.6134 (17)	170 (2)
O3—H3O···O2	0.86 (3)	1.79 (3)	2.6535 (18)	178 (4)
C7—H7···O3^{ii}	0.93	2.57	3.329 (2)	139
C14—H14···O1^{iii}	0.93	2.59	3.395 (2)	145

Symmetry codes: (ii) $x-\frac{1}{2}, y-\frac{1}{2}, z$; (iii) $x+\frac{1}{2}, y+\frac{1}{2}, z$.

The presence of a carboxylic acid group in the molecule of BA is confirmed by the C8—O3, O4 bond lengths of 1.318 (2) and 1.233 (2) Å, respectively. As for the DTBA molecule, the carboxylic acid group is close to co-planar with the benzene ring to which it is bound, forming a dihedral angle of 3.65 (15)°.

3. Supramolecular features

The geometric parameters characterizing the interatomic contacts, as identified in *PLATON* (Spek, 2009), in the crystal of (I) as are given in Table 1. The molecular packing of the crystal structure is mainly governed by hydrogen bonds formed between the carboxylic groups of DTBA and BA, whereby each terminus of the former connects via hydroxy-O—H···O(hydroxy) hydrogen bonds, leading to a non-symmetric, eight-membered {···HOC=O}$_2$ homo-synthon as shown in the two views of Fig. 2(*a*). The resultant three-molecule aggregates are connected through DTBA-C—H···O3(hydroxyl-BA) and BA-C—H···O1(hydroxyl-DTBA)

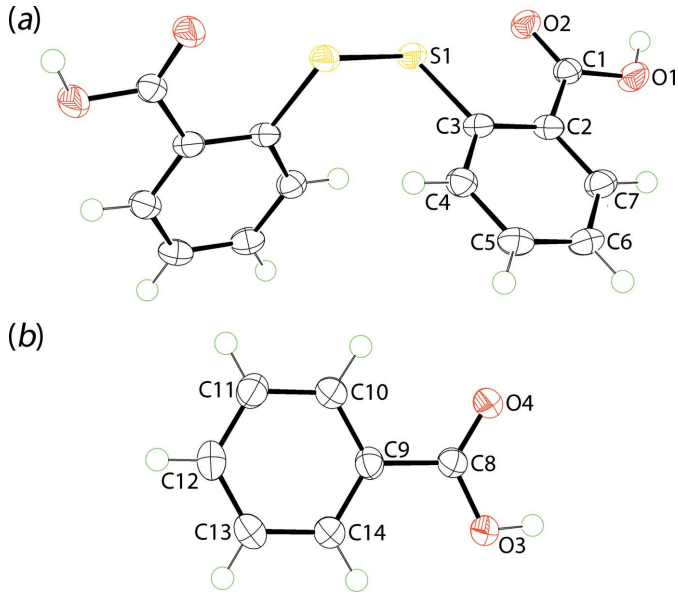

Figure 1
The molecular structures of (*a*) 2,2′-dithiodibenzoic acid and (*b*) benzoic acid in (I), showing the atom-labelling scheme and displacement ellipsoids at the 70% probability level. The molecule in (*a*) is disposed about a twofold axis of symmetry with unlabelled atoms related by the symmetry operation: $1-x, y, \frac{1}{2}-z$.

interactions, to form non-symmetric, ten-membered $\{O\cdots HCCC\}_2$ homo-synthons leading to supramolecular layers in the *ab* plane, Fig. 2(*b*). Owing to the nearly right-angle relationship between the rings in the DTBA molecule, and the co-planarity between the carboxylic acid groups and the respective rings they are connected to, the layers also have a similar topology. Adjacent layers inter-digitate with other layers, on both sides, *i.e.* approximately orthogonally, as highlighted in Fig. 2(*c*). As illustrated in Fig. 2(*d*), the connections between layers are of two types and include π–π stacking interactions between DTBA and BA rings with the inter-centroid (C2–C7)$\cdots$(C9–C14)^{iv} separation being 3.8093 (10) Å, an angle of inclination of 8.36 (8)° and an offset of 1.40 Å for symmetry operation (iv): $1-x, 1-y, 1-z$. The second interaction is a weak, parallel DTBA-hydroxy-O1$\cdots\pi$(C9–C14)^{ii} contact with a O1$\cdots$ring centroid(C9–C14)^{v} separation of 3.9049 (14) Å and angle at O1 = 60.96 (9)° for symmetry operation (v): $\frac{1}{2}-x, \frac{3}{2}-y, 1-z$.

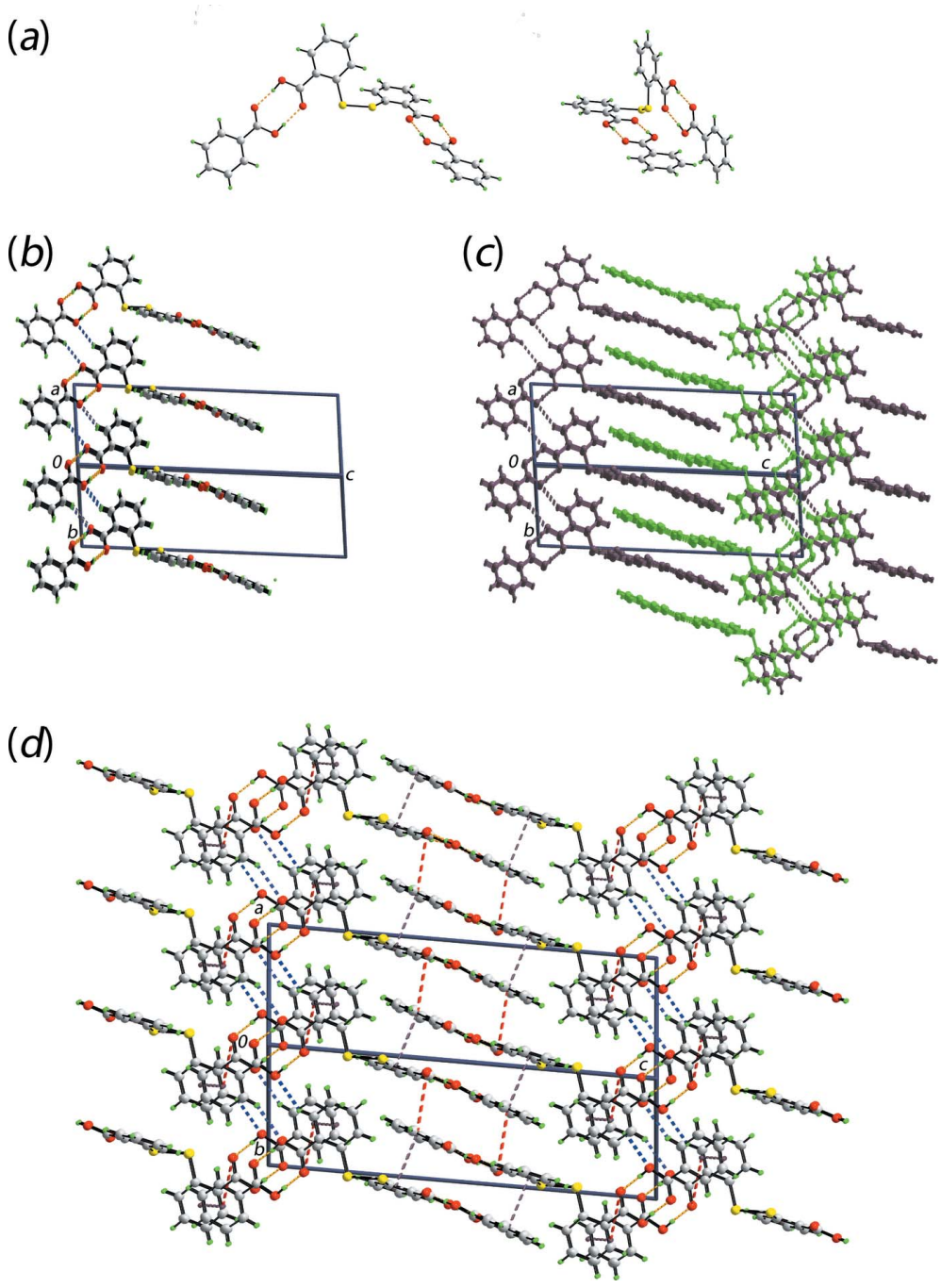

Figure 2
Molecular packing in co-crystal (I): (*a*) two views of the three-molecule aggregate with the the hydroxy-O—H$\cdots$O(carbonyl) hydrogen bonds shown as orange dashed lines, (*b*) supramolecular layer in the *ab* plane where the three-molecule aggregates of (*a*) are linked by DTBA-C—H$\cdots$O(hydroxy-BA), BA-C—H$\cdots$O(hydroxy-DTBA) interactions, shown as blue dashed lines, (*c*) mutual orthogonal inter-digitation of symmetry-related layers and (*d*) a view of the unit-cell contents with π–π and C—O$\cdots\pi$ interactions shown as purple and red dashed lines, respectively.

Table 2
Interaction energies (kJ mol^{-1}) for selected close contacts.

Contact	$E_{electrostatic}$	$E_{polarization}$	$E_{dispersion}$	$E_{exchange\text{-}repulsion}$	E_{total}	Symmetry operation
O3—H3···O2/O1—H1···O4	−126.1	−29.0	−13.1	153.0	−71.7	$1-x, 1-y, 1-z$
*Cg*1(C2–C7)···*Cg*2(C9–C14)	−0.1	−1.5	−41.8	25.5	−21.7	$-x, -y, -z$
*Cg*1(C2–C7)···*Cg*2(C9–C14)	−4.2	−1.3	−30.1	20.8	−18.7	$-\frac{1}{2}+x, \frac{1}{2}+y, z$
C6—H6···S1	−10.2	−2.0	−13.5	15.8	−14.2	$\frac{1}{2}+x, \frac{1}{2}+y, z$
C14—H14···O1/C7—H7···O3	−3.6	−0.9	−13.6	14.8	−7.1	$\frac{1}{2}-x, \frac{1}{2}-y, 1-z$

4. Hirshfeld surface analysis and computational study

To gain better understanding of the nature of the intermolecular interactions identified in (I), the co-crystal and its individual components were subjected to a Hirshfeld surface analysis through the mapping of the normalized contact distance (d_{norm}) as well as calculation of the interaction energies using *CrystalExplorer* (Turner *et al.*, 2017) and in accord with a recent study (Tan & Tiekink, 2018). Briefly, the d_{norm} maps were obtained through the calculation of the internal (d_i) and external (d_e) distances to the nearest nucleus (Spackman & Jayatilaka, 2009), while the interaction energies were calculated using a dispersion-corrected CE-B3LYP/6-31G(d,p) quantum level of theory, as available in *CrystalExplorer* (Turner *et al.*, 2017). The total intermolecular energy is the sum of energies of four main components, comprising electrostatic, polarization, dispersion and exchange-repulsion with scale factors of 1.057, 0.740, 0.871 and 0.618, respectively (Mackenzie *et al.*, 2017).

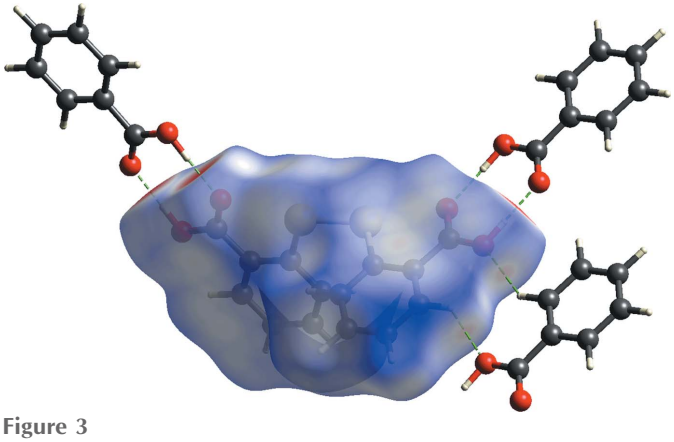

Figure 3
The Hirshfeld surface mapped with d_{norm} for the DTBA molecule in (I) over the range −0.753 to 1.252 a.u., shown interacting with near-neighbour BA molecules connected through hydrogen bonds (green dashed lines).

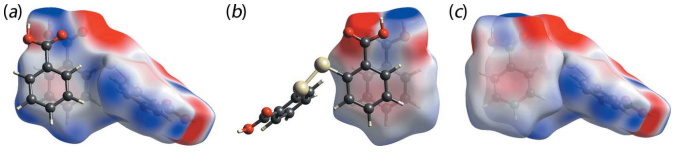

Figure 4
The electrostatic potential mapped over the Hirshfeld surface for (*a*) the DTBA molecule, (*b*) the BA molecule and (*c*) a BA molecule involved in a π–π stacking interaction with the ring of a DTBA molecule. The isovalue was scaled between −0.026 to 0.056 a.u. for all surfaces.

The d_{norm} mapping of the three-molecule aggregate is shown in Fig. 3. In general, the prominent hydrogen-bond interactions are readily identified from the intense red spots on the Hirshfeld surface which are dominated by the strong hydroxy-O—H···O(carbonyl) hydrogen bonds. The calculation of the relevant interaction energies shows that it is the strongest among all of the specified contacts present in the crystal with the calculated (total) energy of −71.7 kJ mol^{-1}, Table 2. By contrast, the diminutive red spots observed around the atoms involved in the benzene-C—H···O(hydroxy) contacts, Table 1, are indicative of weak interactions, and this is confirmed through the calculated interaction energy of merely −7.1 kJ mol^{-1}. The short π–π interaction involving the DTBA and BA benzene rings, mentioned in *Supramolecular features*, has an interaction energy of −21.7 kJ mol^{-1}, *i.e.* more stable than the C—H···O interactions. The energy calculation reveals that such an interaction is mainly dispersive in nature, *cf* Table 2, with the electrostatic character of the corresponding benzene rings being complementary, as demonstrated from the electrostatic surface mapped onto the Hirshfeld surfaces of the individual components of (I), Fig. 4(*a*) and (*b*), and the molecular dimer sustained by π–π contacts in Fig. 4(*c*).

Other important but less significant contacts are noted through the Hirshfeld surface analysis such as a longer π–π interaction between DTBA and BA rings with an inter-centroid (C2–C7)···(C9–C14)^{v} separation of 4.4323 (10) Å, an angle of inclination of 8.36 (8)° and an off-set of 2.74 Å for symmetry operation (v): $\frac{1}{2}-x, \frac{3}{2}-y, 1-z$. In addition, a BA-benzene-C6—H···S contact (2.94 Å) is noted, Table 2.

A quantitative analysis of the Hirshfeld surfaces was performed through the generation of two-dimensional fingerprint plots by combining the d_i and d_e contact distances at the interval of 0.01 Å (McKinnon *et al.*, 2007). The overall fingerprint plot of the co-crystal (DTBA···BA) and the corresponding plots of the individual components are shown

Table 3
Percentage contributions of selected interatomic contacts to the Hirshfeld surface for (I) and for the the individual TDBA and BA molecules.

Contact	Percentage contribution		
	overall	TDBA	BA
H···H	37.0	32.3	41.5
O···H/H···O	21.1	25.3	25.1
S···H/H···S	9.2	12.4	2.1
C···H/H···C	15.3	14.9	12.8
C···C	9.5	9.3	8.7

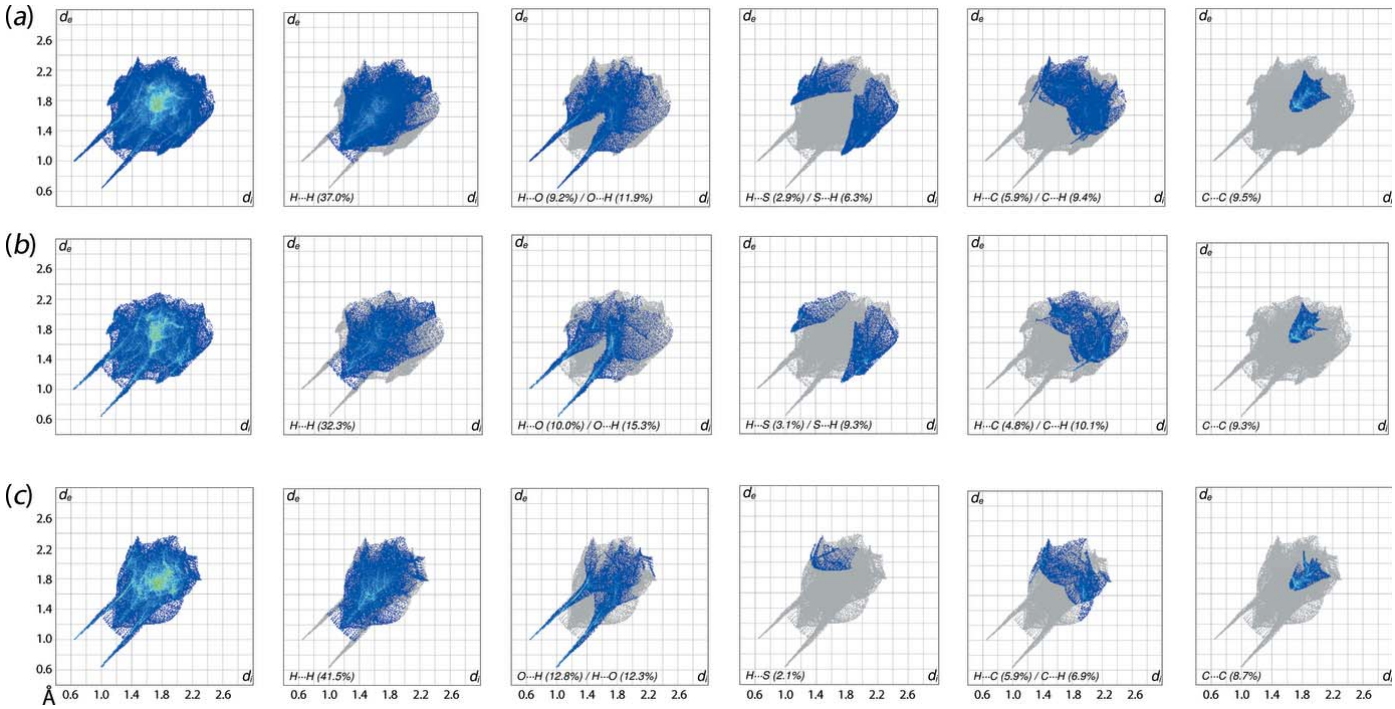

Figure 5
The full two-dimensional fingerprint plot and those delineated into H···H, O···H/H···O, S···H/H···S, C···H/H···C and C···C contacts for (*a*) (I), (*b*) DTBA and (*c*) BA, respectively.

in Fig. 5 and percentage contributions are given in Table 3. In general, the overall bug-like fingerprint profiles of (I) and its individual components very much resemble to each other, as expected for DTBA and BA molecules both with nearly identical donor–acceptor interactions. The major contribution to the overall Hirshfeld surfaces of (I) comprising H···H (37.0%; $d_i + d_e$ ~2.44 Å), O···H/H···O (21.1%; $d_i + d_e$ ~1.64 Å), S···H/H···S (9.2%; $d_i + d_e$ ~2.82 Å) and other contacts (8.0%). Among these contacts, only the O···H/H···O, C···C and S···H/ H···S contacts are shorter than the respective sums of the van der Waals radii to result in meaningful interactions in the crystal, *i.e.* O···H, C···C and S···H = ~1.72, ~3.4 and ~3.0 Å, respectively.

A close inspection on the corresponding decomposed fingerprint plots of the individual DTBA and BA molecules reveals similar compositions as well as $d_i + d_e$ distances except for the O···H/H···O interactions. Thus, overall (I) possesses 11.9% (internal)-O···H-(external) and 9.2% of (internal)-H···O-(external) close contacts as compared to that of 15.3 and 10.0%, respectively, for the individual DTBA molecule, while the individual BA molecule exhibits almost equivalent O···H and H···O contacts, *i.e.* 12.8 *versus* 12.3%. The apparent disparity arises as a result of the larger surface area to volume ratio for the DTBA molecule as compared to the DTBA+BA aggregate when it is considered as a single entity, hence leading to greater exposure of the O···H/H···O contacts in DTBA within its surrounding interacting environment. A smaller disparity is evident for the (internal)-S···H-(external)/(internal)-H···S-(external) contacts, in that the former constitutes about 6.3% in (I) and 9.3% in DTBA, while the latter is about 2.9% in (I) and 3.1% in DTBA, respectively. The BA molecule only exhibits (internal)-H···S-

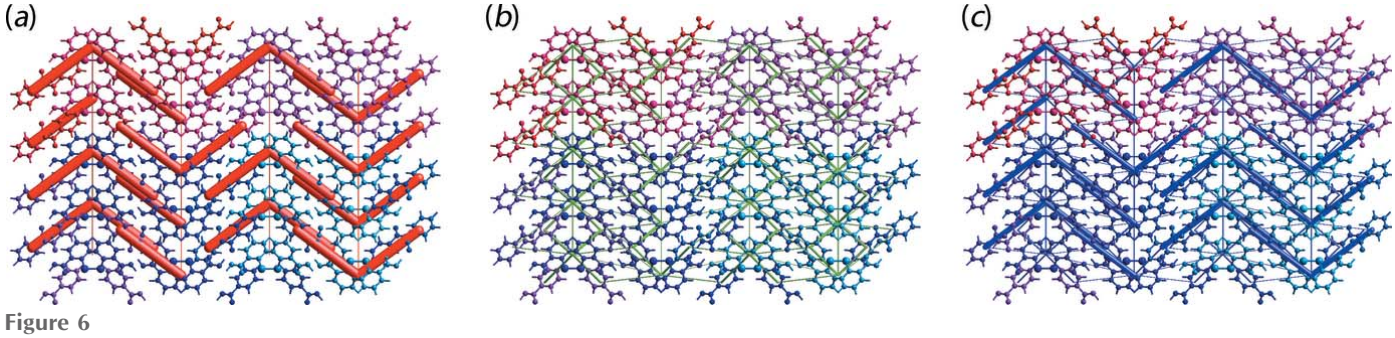

Figure 6
Energy framework of (I) as viewed down along the *a*-axis direction, showing the (*a*) electrostatic potential force, (*b*) dispersion force and (*c*) total energy diagrams. The cylindrical radii are proportional to the relative strength of the corresponding energies and they were adjusted to the same scale factor of 50 with a cut-off value of 5 kJ mol^{-1} within 4 × 4 × 4 unit cells.

Table 4
Experimental details.

Crystal data	
Chemical formula	$C_{14}H_{10}O_4S_2{\cdot}2C_7H_6O_2$
M_r	550.58
Crystal system, space group	Monoclinic, *C*2/*c*
Temperature (K)	100
a, *b*, *c* (Å)	8.2311 (1), 13.3220 (2), 22.7038 (3)
β (°)	95.864 (2)
V (Å^3)	2476.55 (6)
Z	4
Radiation type	Cu $K\alpha$
μ (mm^{-1})	2.41
Crystal size (mm)	0.20 × 0.11 × 0.06
Data collection	
Diffractometer	XtaLAB Synergy, Dualflex, AtlasS2
Absorption correction	Gaussian (*CrysAlis PRO*; Rigaku OD, 2018)
T_{min}, T_{max}	0.643, 1.000
No. of measured, independent and observed [$I > 2\sigma(I)$] reflections	32177, 2589, 2511
R_{int}	0.039
(sin $\theta/\lambda)_{max}$ (Å^{-1})	0.630
Refinement	
$R[F^2 > 2\sigma(F^2)]$, $wR(F^2)$, S	0.039, 0.109, 1.08
No. of reflections	2589
No. of parameters	180
H-atom treatment	H atoms treated by a mixture of independent and constrained refinement
$\Delta\rho_{max}$, $\Delta\rho_{min}$ (e Å^{-3})	0.66, −0.49

Computer programs: *CrysAlis PRO* (Rigaku OD, 2018), *SHELXT* (Sheldrick, 2015*b*), *SHELXL* (Sheldrick, 2015*a*), *ORTEP-3 for Windows* (Farrugia, 2012), *OLEX2* (Dolomanov *et al.*, 2009), *Mercury* (Macrae *et al.*, 2006) and *publCIF* (Westrip, 2010).

(external) contacts that contribute about 2.1% to the overall Hirshfeld surface.

In order to study the overall topology of the energy distributions in the crystal of (I), the energy framework was generated for a cluster of 4 × 4 × 4 unit cells using the same quantum level of theory as mentioned for the interaction energy model. As shown in Fig. 6(*a*)–(*c*), the crystal is significantly governed by electrostatic force owing to the strong O—H···O interactions that result in an alternate V-shape energy topology across the *b*-axis direction. A relatively less significant, but essential dispersion contribution is also observed and arises from the π–π interactions spanning all benzene rings. Overall, it can be concluded that these interacting forces directed the assembly of the molecules in (I).

5. Database survey

As mentioned in the *Structural commentary*, the DTBA molecule is twisted about the central disulfide bond, having a C—S—S—C torsion angle of −83.19 (8)°. A survey of the literature indicates that this is a common feature of such molecules. A search of the Cambridge Structural Database (Version 5.39; Groom *et al.*, 2016), indicates there are 33 different molecules of DTBA. The C—S—S—C torsion angles span a range of approximately 20° with the narrowest angle of 80.06 (9)° found in the structure of a 1:1 co-crystal of DTBA with *trans*-1,2-bis(4-pyridyl)ethene (Broker & Tiekink, 2007) and the widest angle of 100.98 (17)° was observed in in a co-crystal salt, *i.e.* $[NH_4]$[DTBA_H]DBTA (Murugavel *et al.*, 2001).

6. Synthesis and crystallization

All chemicals were of reagent grade and used as received without purification. 2-Thiobenzoic acid (Merck; 0.154 g, 0.001 mol) was mixed with benzoic acid (R&M; 0.122 g, 0.001 mol) and ground for 15 minutes in the presence of a few drops of methanol. The procedure was repeated three times. Colourless blocks were obtained by carefully layering toluene (1 ml) on an *N*,*N*-dimethylformamide (1 ml) solution of the ground mixture. M.p. 384.2–385.6 K. IR (cm^{-1}): 3070 ν(C—H), 1677 ν(C═O), 1584 ν(C═C), 1415 δ(C—H), 706 δ(C═C), 684 δ(OCO).

7. Refinement

Crystal data, data collection and structure refinement details are summarized in Table 4. The carbon-bound H atoms were placed in calculated positions (C—H = 0.93 Å) and were included in the refinement in the riding-model approximation, with U_{iso}(H) set to 1.2U_{eq}(C). The oxygen-bound H atoms were located from difference-Fourier maps and refined without constraint.

Funding information

The support of Sunway University for studies in co-crystals, through Grant No. INT-FST-RCCM-2016–01, is gratefully acknowledged.

References

Allen, F. H., Motherwell, W. D. S., Raithby, P. R., Shields, G. P. & Taylor, R. (1999). *New J. Chem.* pp. 25–34.
Broker, G. A. & Tiekink, E. R. T. (2007). *CrystEngComm*, **9**, 1096–1109.
Dolomanov, O. V., Bourhis, L. J., Gildea, R. J., Howard, J. A. K. & Puschmann, H. (2009). *J. Appl. Cryst.* **42**, 339–341.
Duggirala, N. K., Wood, G. P. F., Fischer, A., Wojtas, Ł., Perry, M. L. & Zaworotko, M. J. (2015). *Cryst. Growth Des.* **15**, 4341–4354.
Farrugia, L. J. (2012). *J. Appl. Cryst.* **45**, 849–854.
Gorobet, A., Vitiu, A., Petuhov, O. & Croitor, L. (2018). *Polyhedron*, **151**, 51–57.
Groom, C. R., Bruno, I. J., Lightfoot, M. P. & Ward, S. C. (2016). *Acta Cryst.* B**72**, 171–179.
Mackenzie, C. F., Spackman, P. R., Jayatilaka, D. & Spackman, M. A. (2017). *IUCrJ*, **4**, 575–587.
Macrae, C. F., Edgington, P. R., McCabe, P., Pidcock, E., Shields, G. P., Taylor, R., Towler, M. & van de Streek, J. (2006). *J. Appl. Cryst.* **39**, 453–457.
McKinnon, J. J., Jayatilaka, D. & Spackman, M. A. (2007). *Chem. Commun.* pp. 3814.
Meng, X.-G., Xiao, Y.-L., Zhang, H. & Zhou, C.-S. (2008). *Acta Cryst.* C**64**, o261–o263.
Murugavel, R., Baheti, K. & Anantharaman, G. (2001). *Inorg. Chem.* **40**, 6870–6878.
Nakanishi, W., Nakamoto, T., Hayashi, S., Sasamori, T. & Tokitoh, N. (2007). *Chem. Eur. J.* **13**, 255–268.

Rigaku OD (2018). *CrysAlis PRO*. Rigaku Corporation, Oxford, UK.
Seaton, C. C. (2011). *CrystEngComm*, **13**, 6583–6592.
Shattock, T. R., Arora, K. K., Vishweshwar, P. & Zaworotko, M. J. (2008). *Cryst. Growth Des.* **8**, 4533–4545.
Sheldrick, G. M. (2015*a*). *Acta Cryst.* A**71**, 3–8.
Sheldrick, G. M. (2015*b*). *Acta Cryst.* C**71**, 3–8.
Spackman, M. A. & Jayatilaka, D. (2009). *CrystEngComm*, **11**, 19–32.
Spek, A. L. (2009). *Acta Cryst.* D**65**, 148–155.
Steiner, T. (2001). *Acta Cryst.* B**57**, 103–106.
Tan, S. L. & Tiekink, E. R. T. (2018). *Acta Cryst.* E**74**, 1764–1771.
Tan, S. L. & Tiekink, E. R. T. (2019). *Z. Kristallogr. New Cryst. Struct.* **234**; https://doi:org/10.1515/ncrs-2018-0442.
Turner, M. J., Mckinnon, J. J., Wolff, S. K., Grimwood, D. J., Spackman, P. R., Jayatilaka, D. & Spackman, M. A. (2017). *CrystalExplorer17*. The University of Western Australia.
Westrip, S. P. (2010). *J. Appl. Cryst.* **43**, 920–925.

supporting information

Acta Cryst. (2019). E**75**, 1-7 [https://doi.org/10.1107/S2056989018017097]

A 1:2 co-crystal of 2,2′-dithiodibenzoic acid and benzoic acid: crystal structure, Hirshfeld surface analysis and computational study

Sang Loon Tan and Edward R. T. Tiekink

Computing details

Data collection: *CrysAlis PRO* (Rigaku OD, 2018); cell refinement: *CrysAlis PRO* (Rigaku OD, 2018); data reduction: *CrysAlis PRO* (Rigaku OD, 2018); program(s) used to solve structure: SHELXT (Sheldrick, 2015*b*); program(s) used to refine structure: *SHELXL* (Sheldrick, 2015*a*); molecular graphics: *ORTEP-3 for Windows* (Farrugia, 2012), OLEX2 (Dolomanov *et al.*, 2009) and *Mercury* (Macrae *et al.*, 2006); software used to prepare material for publication: *publCIF* (Westrip, 2010).

2,2′-Dithiodibenzoic acid–benzoic acid (1/2)

Crystal data

$C_{14}H_{10}O_4S_2{\cdot}2C_7H_6O_2$
M_r = 550.58
Monoclinic, *C*2/*c*
a = 8.2311 (1) Å
b = 13.3220 (2) Å
c = 22.7038 (3) Å
β = 95.864 (2)°
V = 2476.55 (6) Å^3
Z = 4
F(000) = 1144
D_x = 1.477 Mg m^{-3}
Cu *Kα* radiation, *λ* = 1.54184 Å
Cell parameters from 18092 reflections
θ = 3.9–76.2°
μ = 2.41 mm^{-1}
T = 100 K
Prism, colourless
0.20 × 0.11 × 0.06 mm

Data collection

XtaLAB Synergy, Dualflex, AtlasS2 diffractometer
Radiation source: micro-focus sealed X-ray tube, PhotonJet (Cu) X-ray Source
Mirror monochromator
Detector resolution: 5.2558 pixels mm^{-1}
ω scans
Absorption correction: gaussian (CrysAlis PRO; Rigaku OD, 2018)
T_{min} = 0.643, T_{max} = 1.000
32177 measured reflections
2589 independent reflections
2511 reflections with $I > 2\sigma(I)$
R_{int} = 0.039
θ_{max} = 76.2°, θ_{min} = 3.9°
h = −10→10
k = −16→16
l = −28→28

Refinement

Refinement on F^2
Least-squares matrix: full
$R[F^2 > 2\sigma(F^2)]$ = 0.039
$wR(F^2)$ = 0.109
S = 1.08
2589 reflections
180 parameters
0 restraints
Primary atom site location: dual
Hydrogen site location: mixed
H atoms treated by a mixture of independent and constrained refinement
$w = 1/[\sigma^2(F_o^2) + (0.0597P)^2 + 4.0853P]$ where $P = (F_o^2 + 2F_c^2)/3$

$(\Delta/\sigma)_{max}$ = 0.001
$\Delta\rho_{max}$ = 0.66 e Å^{-3}
$\Delta\rho_{min}$ = −0.49 e Å^{-3}

Special details

Geometry. All esds (except the esd in the dihedral angle between two l.s. planes) are estimated using the full covariance matrix. The cell esds are taken into account individually in the estimation of esds in distances, angles and torsion angles; correlations between esds in cell parameters are only used when they are defined by crystal symmetry. An approximate (isotropic) treatment of cell esds is used for estimating esds involving l.s. planes.

Fractional atomic coordinates and isotropic or equivalent isotropic displacement parameters (Å²)

	x	*y*	*z*	U_{iso}*/U_{eq}
S1	0.50125 (5)	0.53534 (3)	0.29507 (2)	0.01870 (14)
O1	0.29643 (16)	0.49404 (10)	0.46525 (5)	0.0239 (3)
H1o	0.328 (3)	0.544 (2)	0.4890 (12)	0.042 (7)*
O2	0.46078 (15)	0.57402 (9)	0.40809 (5)	0.0213 (3)
O3	0.52518 (17)	0.72548 (10)	0.48274 (6)	0.0260 (3)
H3o	0.502 (4)	0.676 (2)	0.4589 (13)	0.053 (8)*
O4	0.35583 (16)	0.64485 (9)	0.53788 (5)	0.0237 (3)
C1	0.3639 (2)	0.50608 (12)	0.41556 (7)	0.0179 (3)
C2	0.3123 (2)	0.43148 (12)	0.36912 (7)	0.0175 (3)
C3	0.3622 (2)	0.43865 (12)	0.31172 (7)	0.0172 (3)
C4	0.3046 (2)	0.36819 (13)	0.26917 (7)	0.0192 (3)
H4	0.336143	0.372512	0.231068	0.023*
C5	0.2004 (2)	0.29140 (13)	0.28321 (8)	0.0213 (4)
H5	0.162961	0.244879	0.254423	0.026*
C6	0.1519 (2)	0.28379 (13)	0.33971 (8)	0.0220 (4)
H6	0.083137	0.232083	0.349054	0.026*
C7	0.2070 (2)	0.35389 (13)	0.38213 (8)	0.0208 (3)
H7	0.173415	0.349359	0.419926	0.025*
C8	0.4462 (2)	0.71641 (13)	0.53011 (7)	0.0195 (3)
C9	0.4761 (2)	0.79789 (13)	0.57426 (7)	0.0196 (3)
C10	0.4020 (2)	0.79189 (13)	0.62667 (7)	0.0212 (4)
H10	0.331481	0.739174	0.632630	0.025*
C11	0.4340 (2)	0.86479 (14)	0.66992 (8)	0.0234 (4)
H11	0.384929	0.860972	0.704986	0.028*
C12	0.5395 (2)	0.94372 (14)	0.66082 (8)	0.0238 (4)
H12	0.561938	0.992032	0.690087	0.029*
C13	0.6111 (2)	0.95056 (14)	0.60843 (8)	0.0247 (4)
H13	0.680059	1.004025	0.602298	0.030*
C14	0.5801 (2)	0.87766 (13)	0.56496 (8)	0.0225 (4)
H14	0.628625	0.882052	0.529801	0.027*

Atomic displacement parameters (Å²)

	U^{11}	U^{22}	U^{33}	U^{12}	U^{13}	U^{23}
S1	0.0254 (2)	0.0140 (2)	0.0171 (2)	−0.00272 (14)	0.00424 (16)	−0.00104 (13)
O1	0.0350 (7)	0.0198 (6)	0.0178 (6)	−0.0079 (5)	0.0079 (5)	−0.0026 (5)
O2	0.0281 (6)	0.0181 (6)	0.0184 (6)	−0.0062 (5)	0.0054 (5)	−0.0024 (4)

O3	0.0380 (8)	0.0203 (6)	0.0212 (6)	−0.0079 (5)	0.0110 (5)	−0.0048 (5)
O4	0.0312 (7)	0.0193 (6)	0.0212 (6)	−0.0069 (5)	0.0062 (5)	−0.0025 (5)
C1	0.0218 (8)	0.0153 (8)	0.0169 (8)	0.0010 (6)	0.0027 (6)	0.0012 (6)
C2	0.0211 (8)	0.0132 (8)	0.0181 (8)	0.0005 (6)	0.0006 (6)	−0.0002 (6)
C3	0.0202 (8)	0.0120 (7)	0.0193 (8)	0.0003 (6)	0.0014 (6)	0.0006 (6)
C4	0.0221 (8)	0.0171 (8)	0.0184 (8)	−0.0002 (6)	0.0023 (6)	−0.0014 (6)
C5	0.0238 (8)	0.0159 (8)	0.0238 (8)	−0.0017 (6)	−0.0001 (6)	−0.0037 (6)
C6	0.0247 (8)	0.0147 (8)	0.0266 (9)	−0.0039 (7)	0.0022 (7)	0.0002 (6)
C7	0.0258 (8)	0.0169 (8)	0.0201 (8)	−0.0012 (7)	0.0033 (6)	0.0016 (6)
C8	0.0228 (8)	0.0173 (8)	0.0186 (8)	−0.0006 (6)	0.0027 (6)	0.0008 (6)
C9	0.0238 (8)	0.0163 (8)	0.0184 (8)	0.0008 (6)	0.0010 (6)	−0.0004 (6)
C10	0.0233 (8)	0.0186 (8)	0.0219 (8)	−0.0009 (6)	0.0030 (6)	0.0011 (6)
C11	0.0269 (9)	0.0235 (9)	0.0200 (8)	0.0015 (7)	0.0033 (7)	−0.0016 (7)
C12	0.0279 (9)	0.0197 (8)	0.0232 (9)	0.0015 (7)	−0.0006 (7)	−0.0048 (7)
C13	0.0276 (9)	0.0183 (8)	0.0282 (9)	−0.0035 (7)	0.0026 (7)	−0.0012 (7)
C14	0.0272 (9)	0.0198 (8)	0.0212 (8)	−0.0028 (7)	0.0051 (7)	−0.0008 (7)

Geometric parameters (Å, º)

S1—S1^{i}	2.0446 (8)	C6—H6	0.9300
S1—C3	1.7889 (17)	C6—C7	1.384 (2)
O1—H1o	0.88 (3)	C7—H7	0.9300
O1—C1	1.317 (2)	C8—C9	1.481 (2)
O2—C1	1.229 (2)	C9—C10	1.393 (2)
O3—H3o	0.87 (3)	C9—C14	1.395 (2)
O3—C8	1.318 (2)	C10—H10	0.9300
O4—C8	1.233 (2)	C10—C11	1.387 (2)
C1—C2	1.479 (2)	C11—H11	0.9300
C2—C3	1.409 (2)	C11—C12	1.393 (3)
C2—C7	1.400 (2)	C12—H12	0.9300
C3—C4	1.395 (2)	C12—C13	1.383 (3)
C4—H4	0.9300	C13—H13	0.9300
C4—C5	1.393 (2)	C13—C14	1.390 (3)
C5—H5	0.9300	C14—H14	0.9300
C5—C6	1.385 (2)		
C3—S1—S1^{i}	105.68 (6)	C6—C7—H7	119.4
C1—O1—H1o	107.9 (18)	O3—C8—C9	115.08 (15)
C8—O3—H3o	110 (2)	O4—C8—O3	122.88 (16)
O1—C1—C2	114.38 (14)	O4—C8—C9	122.04 (15)
O2—C1—O1	122.96 (15)	C10—C9—C8	118.64 (16)
O2—C1—C2	122.65 (15)	C10—C9—C14	120.14 (16)
C3—C2—C1	121.58 (15)	C14—C9—C8	121.19 (15)
C7—C2—C1	119.01 (15)	C9—C10—H10	120.1
C7—C2—C3	119.38 (15)	C11—C10—C9	119.78 (17)
C2—C3—S1	119.84 (12)	C11—C10—H10	120.1
C4—C3—S1	121.18 (13)	C10—C11—H11	120.0
C4—C3—C2	118.96 (15)	C10—C11—C12	119.96 (17)

C3—C4—H4	119.7	C12—C11—H11	120.0
C5—C4—C3	120.63 (16)	C11—C12—H12	119.9
C5—C4—H4	119.7	C13—C12—C11	120.29 (17)
C4—C5—H5	119.7	C13—C12—H12	119.9
C6—C5—C4	120.52 (16)	C12—C13—H13	120.0
C6—C5—H5	119.7	C12—C13—C14	120.09 (17)
C5—C6—H6	120.3	C14—C13—H13	120.0
C7—C6—C5	119.36 (16)	C9—C14—H14	120.1
C7—C6—H6	120.3	C13—C14—C9	119.73 (16)
C2—C7—H7	119.4	C13—C14—H14	120.1
C6—C7—C2	121.15 (16)		

Symmetry code: (i) $-x+1, y, -z+1/2$.

Hydrogen-bond geometry (Å, º)

D—H···*A*	*D*—H	H···*A*	*D*···*A*	*D*—H···*A*
O1—H1O···O4	0.88 (3)	1.74 (3)	2.6134 (17)	170 (2)
O3—H3O···O2	0.86 (3)	1.79 (3)	2.6535 (18)	178 (4)
C7—H7···O3^{ii}	0.93	2.57	3.329 (2)	139
C14—H14···O1^{iii}	0.93	2.59	3.395 (2)	145

Symmetry codes: (ii) $x-1/2, y-1/2, z$; (iii) $x+1/2, y+1/2, z$.